communications earth & environment

Article

A Nature Portfolio journal

https://doi.org/10.1038/s43247-026-03344-y

# Colony formation sustains the global competitiveness of nitrogen-fixing *Trichodesmium* under ocean acidification



Weicheng Luo [1,2,3], Meri Eichner [2], Ondřej Prášil [2], Futing Zhang [2], Keisuke Inomura [4] & Ya-Wei Luo [1,5]

Anthropogenic carbon dioxide emissions drive ocean acidification. *Trichodesmium*, a key marine nitrogen-fixing cyanobacterium, displays contrasting growth responses to ocean acidification across morphotypes: negative in filamentous free trichomes but neutral or positive in colonies. However, lacking mechanistic understanding for these discrepancies has impaired our ability to predict *Trichodesmium*'s ecophysiological response. Here, we develop ecophysiological models to underpin mechanisms behind these divergent responses. For free trichomes, ocean acidification reduces nitrogen-fixing enzyme activity and photosynthetic energy production. In colonies, however, it alleviates copper and ammonia toxicity within the microenvironment—likely synergizing with enhanced iron acquisition—thereby outweighing minor benefit from relieved inorganic carbon limitation in the colony center. Projections suggest that globally, ocean acidification will reduce nitrogen fixation of trichomes by 16 ± 6% but increase that of colonies by 19 ± 24% within this century. By resolving morphotype-specific mechanisms, our study clarifies *Trichodesmium*'s adaptive strategies for sustaining its competitiveness and biogeochemical impacts in the changing ocean.

Ocean acidification (OA), driven by anthropogenic $CO_2$ emission and its subsequent dissolution into seawater[1], poses physiological challenges to marine microbes. These can include the disruption of cellular proton gradients, increased energy demands for homeostasis, and the potential induction of oxidative stress[2–4]. Biological $N_2$ fixation is an essential process that fuels a large fraction of primary production in the ocean[5]. *Trichodesmium* is a globally prominent autotrophic $N_2$-fixing cyanobacterium, widely distributed in tropical and subtropical oceans[6–8]. Given its important contribution to global $N_2$ fixation (60–80 Tg N $yr^{-1}$)[9–11], understanding how *Trichodesmium* responds to climate change effects of OA is critical.

*Trichodesmium* can exist freely consisting of dozens of cells (trichome), or aggregate into colonies composed of tens to hundreds of trichomes, typically forming spherical ("puff") or fusiform ("tuft") morphologies[6]. Colony formation, which can be induced by nutrient limitation[12] and facilitated by physical interactions between trichomes[13], imparts several ecological advantages to *Trichodesmium*[14]. These include enhancing access to insoluble nutrients such as dust-derived iron[15], regulating buoyancy to maintain optimal light exposure at the sea surface[16], and reducing grazing pressure from zooplankton[17]. High occurrences of both free trichomes and colonies of *Trichodesmium* and their substantial contribution to $N_2$ fixation have been reported in oligotrophic oceans[14,18].

Accumulating evidence suggests that free trichomes and colonies of *Trichodesmium* may respond differently to OA. Free trichomes of *Trichodesmium* are most likely to respond negatively to OA. While a range of early studies using artificial YBCII media for growing *Trichodesmium* free trichomes showed strong positive effects of OA[19–22], more recent culture experiments with seawater-based Aquil-media, lowering possible contamination such as from ammonium, have shown that OA can decrease the $N_2$ fixation and growth rates of the trichomes[2,23–25]. Previous laboratory and modeling studies indicate that while OA may benefit *Trichodesmium* by reducing energy expenditure of its carbon concentrating mechanism (CCM) due to elevated $CO_2$, this advantage is typically outweighed by negative effects of low pH[2,26]. The primary physiological impacts include diminished energy production from photosynthetic electron transfer (PET) and reduced efficiency of nitrogenase (the enzyme for $N_2$ fixation), which can be attributed to proton imbalance, impaired ATP synthesis efficiency, and potentially intensified stress resulting from oxygen management due to decreased carbon fixation[2,24,27]. However, these studies were mostly based on

[1]State Key Laboratory of Marine Environmental Science and College of Ocean and Earth Sciences, Xiamen University, Xiamen, China. [2]Centre Algatech, Institute of Microbiology of the Czech Academy of Sciences, Třeboň, Czechia. [3]Institute for Advanced Study & College of Life Sciences and Oceanography, Shenzhen University, Shenzhen, China. [4]Graduate School of Oceanography, University of Rhode Island, Narragansett, RI, USA. [5]China-ASEAN College of Marine Sciences, Xiamen University Malaysia, Sepang, Selangor, Malaysia. e-mail: ywluo@xmu.edu.cn

the daily average status of *Trichodesmium* trichome and ignored its diel physiological dynamics.

Conversely, studies using natural seawater reported that natural *Trichodesmium* colonies showed no response[28], or even enhanced growth and $N_2$ fixation under OA[29–31]. Although the reasons are still unclear, this contrasting response of *Trichodesmium* colonies to OA may stem from the distinct chemical microenvironment within colonies[30]. For example, attributing to elevated cell density in *Trichodesmium* colonies, dissolved inorganic carbon (DIC) concentration within *Trichodesmium* colonies can be reduced substantially during periods with active photosynthesis and this results in DIC limitation[32]. This DIC limitation is particularly pronounced in the colony center, where the diffusion distance to the DIC-saturated surrounding water is greatest. Elevated $CO_2$ under OA could therefore alleviate the carbon limitation for photosynthesis in these interior regions. Additionally, due to DIC consumption during photosynthesis, the microenvironmental pH levels within *Trichodesmium* colonies can increase by up to 0.6 units[30]. These diel changes are substantial compared to the projected decrease under OA[1]. This highlights the highly dynamic feature of pH fluctuations at the microscale, which may mitigate the low-pH stress on photosynthetic ATP production and nitrogenase efficiency imposed by OA. Such internal pH buffering also suggests an adaptive capability of *Trichodesmium* in natural seawater, where carbonate chemistry varies over multiple timescales ranging from diel to geological. Overall, systematic and quantitative understanding remains limited regarding how diurnal interactions between the colonial microenvironment and intracellular physiological processes promote *Trichodesmium* growth under OA while overcoming other OA-induced stressors.

The response of *Trichodesmium* to OA can also be modulated by iron (Fe), a micronutrient highly required by $N_2$ fixers, including *Trichodesmium*[23,33,34]. Unlike other marine diazotrophs, *Trichodesmium* conducts both $N_2$ fixation and photosynthesis concurrently during daylight. Its carbon fixation peaks early in the light period before declining and stabilizing during midday, when $N_2$ fixation mainly occurs[35]. This down-regulation of carbon fixation is mainly achieved through high respiration activity, which reduces the plastoquinone pool and sends negative feedback to photosystem II. The resulting decrease in photosynthetic $O_2$ production and carbon fixation helps protect nitrogenase from $O_2$ inhibition[35]. As the enzymes involving both processes contain substantial amount of Fe, the intracellular Fe allocation strategy is critical for *Trichodesmium*'s survival.

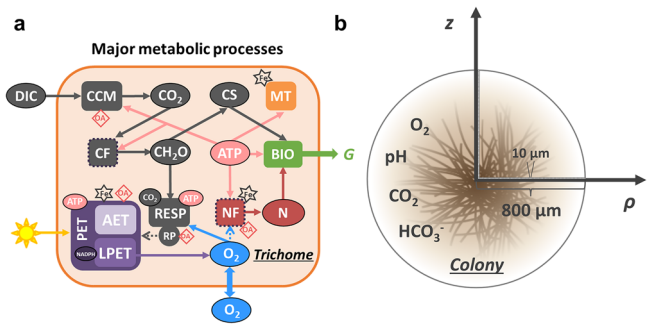


**Fig. 1 | Model framework of *Trichodesmium* trichome and colony. a** The intracellular physiological processes and the effects of ocean acidification (OA) in the *Trichodesmium* trichome model. The simplified plot neglects the NADPH consumption by carbon and $N_2$ fixations (dashed frames), as well as the connection from ATP production to its consumption. The black pentagrams and the red diamonds mark Fe-requiring and OA-impacting metabolic processes, respectively. Dashed arrows represent inhibition effects. CF carbon fixation, $CH_2O$ carbohydrate, CS carbon skeleton, RESP ordinary respiration, RP respiratory protection, NF $N_2$ fixation, N fixed nitrogen, MT maintenance, BIO biosynthesis, G growth rate. **b** Schematic diagram of the microenvironment of modeled colony. This framework was established using a finite difference method with the radius (800 μm) of the colony divided into 80 equal parts, with the cell density ($\rho$) decreasing with the increasing distance ($z$) to colony center.

OA can change this Fe allocation. For example, both laboratory experiments[2,23] and an ecophysiological model[26] have demonstrated that more intracellular Fe in *Trichodesmium* trichomes is allocated to nitrogenase to compensate its lowered efficiency under OA. Hence, when this compensation via reallocating intracellular Fe is restricted by limiting Fe supplies, the negative OA effects to *Trichodesmium* can be more severe[2,26]. These studies suggest that dynamic intracellular Fe allocation can be involved in *Trichodesmium*'s strategy in dealing with OA effects.

Considering collectively the microenvironmental and physiological characteristics in colonies, we hypothesize that the opposite responses of *Trichodesmium* free trichomes and colonies to OA result from the different diurnal dynamics of $CO_2$ and pH in the trichome's and the colony's immediate extracellular microenvironment, which consequently impacts DIC supply and intracellular Fe allocation. However, this hypothesis has not been tested through direct comparisons between trichomes and colonies under identical conditions. To test this hypothesis, we constructed two ecophysiological models. The first model simulates a free *Trichodesmium* trichome in a constant extracellular environment, based on evidence that chemical variations around free trichome are minimal (typically <0.5% compared to the bulk environment)[36]. The second model simulates a puff-shaped *Trichodesmium* colony with an explicit dynamic microenvironment, where key chemical properties ($O_2$ and carbonate system parameters, including $CO_2$, $HCO_3^-$, and pH) vary temporally and spatially due to cellular metabolic activities. The models simulated the diurnal rhythms of cellular processes in order to resolve diurnal dynamics in the microenvironment and to address their role in modulating the response of *Trichodesmium* to OA.

## Results and discussion

### General model framework

The *Trichodesmium* trichome model was constructed based on several previous models of *Trichodesmium*, integrating their schemes of physiological OA effects[26] with diurnal dynamics of core metabolic processes regulated by intracellular $O_2$ management and Fe allocations[27,37] (Fig. 1a). Briefly, the trichome model simulated key physiological processes including PET, CCM, carbon fixation, $N_2$ fixation, and maintenance. Light-regulated PET, producing adenosine triphosphate (ATP) and nicotinamide adenine dinucleotide phosphate hydrogen (NADPH), which were allocated to constrain the rates of other physiological processes. The allocation of intracellular Fe to various physiological processes also limited the rates of these processes. OA impacted the Fe allocations, impaired ATP production, changed ATP consumption, and lowered nitrogenase efficiency. $N_2$ fixation was also regulated by intracellular $O_2$ level.

The *Trichodesmium* colony model was set up by further integrating the trichome model to a framework simulating the colony's extracellular microenvironment (Fig. 1b). The modeled colony with a radius of 800 μm was divided into 80 equal grids from its center to its periphery[38]. It was assumed that all filamentous trichomes within the modeled puff-shaped colony passed through its central region with a radius of 800 μm. Despite the higher cell density in the central region of the colony, this circular grid configuration ensured a relatively uniform biomass distribution across all grid segments[36]. This spatial arrangement enabled the comparison of modeled biomass-specific rates between grid sectors to provide a reliable approximation of variations in total metabolic rates. In the colony's microenvironment, defined in this study as the sphere that the colony expands, the extracellular chemical properties, including concentrations of $O_2$ and carbonate system (pH, $CO_2$, and $HCO_3^-$) were dynamically simulated as results of biological production and consumption, chemical reactions, and physical diffusion.

The spatial segregation of carbon fixation and $N_2$ fixation into different *Trichodesmium* cells were not considered in both the trichome and the colony models, as the existence of the segregation still remains questionable[37,39].

Both the trichome and colony models ran over a 12-h diurnal period with dynamic light intensity, while the accumulated organic carbon and

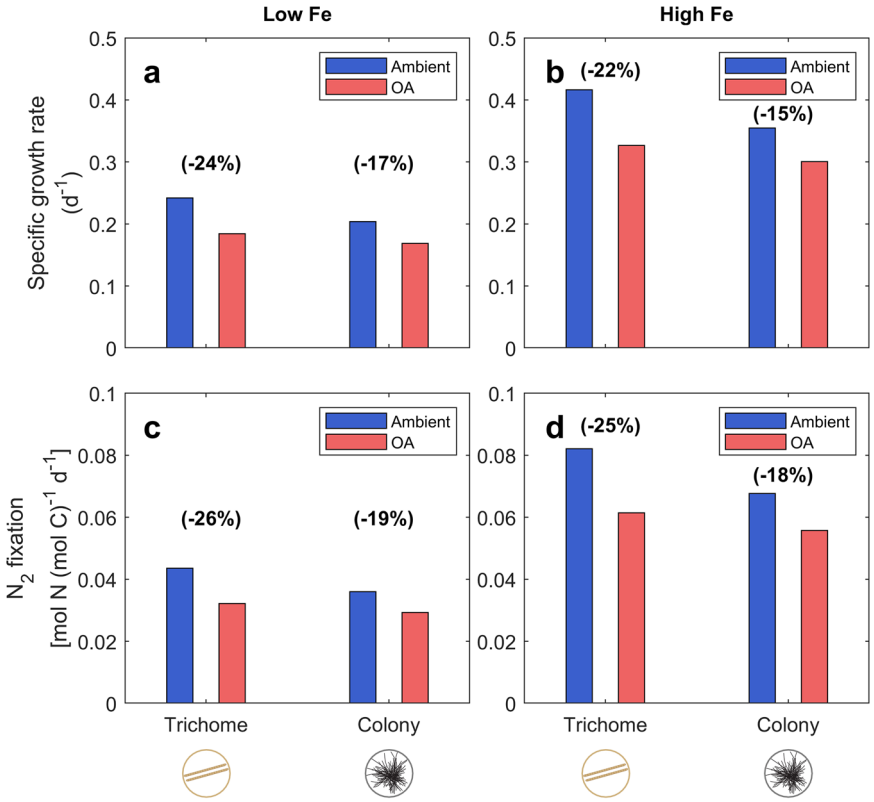


**Fig. 2 | Simulated growth rates and daily-integrated $N_2$ fixation rates of *Trichodesmium* free trichome and colony under limiting Fe and replete Fe conditions.** **a**, **b** The comparison of growth rates under ambient and acidified (OA) conditions. **c**, **d** The comparison of $N_2$ fixation rates under ambient and OA conditions. The sketch of *Trichodesmium* colony was modified from Klawonn et al. [36].

nitrogen at the end of the period were used to calculate the rate of biomass syntheses. The simulations were conducted under ambient (pH = 8.08, $pCO_2$ = 380 ppm) or OA (pH = 7.88, $pCO_2$ = 750 ppm) conditions, while the far-field environmental dissolved inorganic Fe (Fe′) concentration being either limited (40 pM) or replete (1250 pM). All pH values were reported on the total scale. The levels of pH, $pCO_2$ and Fe′ used in this study were selected based on the experimental setup in Shi et al. [23].

Most model parameters were adopted from previous studies or tuned by fitting model results to experimental observations. Meanwhile, several key model parameters were optimized to maximize modeled growth rate at each simulation condition, implicitly assuming that *Trichodesmium* adjusts its metabolic processes to grow optimally in response to changes in environmental conditions.

More details of the model structure and parameters are described in METHODS and Supplementary Note 1.

### Simulated growth and $N_2$ fixation rates of free *Trichodesmium* trichome

The results of the *Trichodesmium* free trichome model showed that OA reduced the daily growth and $N_2$ fixation rates by approximately 24% and 26%, respectively, when Fe is limiting (Fig. 2 and Supplementary Table 1). Replete Fe considerably promoted the modeled growth and $N_2$ fixation rates, while only slightly mitigated the negative impacts of OA to 22% and 25%, respectively (Fig. 2 and Supplementary Table 1). Additionally, when comparing the diurnal variations of the model results under limiting-Fe and replete-Fe conditions, the patterns were similar, although differing in magnitude (Fig. 3 and Supplementary Fig. 1). We thereby focused on presenting and analyzing the results under Fe limitation hereafter, unless specified otherwise.

OA did not greatly alter the overall diurnal rhythms of gross carbon fixation and $N_2$ fixation in the modeled trichome compared to ambient condition (Fig. 3a, b). However, it markedly reduced the rates of both processes. Specifically, OA lowered gross carbon fixation, particularly during the early-light peak in activity (Fig. 3a). It also substantially decreased $N_2$ fixation during the middle light period, when low intracellular $O_2$ levels (Supplementary Fig. 2a) allowed $N_2$ fixation activity (Fig. 3b). Notably, OA slightly shortened the duration of this low-$O_2$ window (Supplementary Fig. 2a), implying that intracellular $O_2$ management may be involved in modulating the responses of *Trichodesmium* trichomes to OA (*see* discussion later).

### Simulated growth and $N_2$ fixation rates of *Trichodesmium* colony

In the *Trichodesmium* colony model, OA reduced the growth and $N_2$ fixation rates by 17% and 19%, respectively (Fig. 2 and Supplementary Table 1), slightly less than those in the single trichome model. The simulated carbon and $N_2$ fixation rates in the colony displayed similar temporal patterns to those in the trichome (Fig. 3a–d). These temporal variations were further overlaid by substantial spatial variations, spanning from the colony center to its periphery (Fig. 3e–h).

We first analyzed the modeled carbon fixation rates in two stages of the light period. During the early light period (0−3 h) with peak carbon fixation rates (Fig. 3c), the interplay of DIC consumption by the colony and DIC diffusion from the surrounding seawater resulted in steep gradients with lower $CO_2$ and $HCO_3^-$ concentrations near the colony center (Figs. 3e, g, 4g–j and Supplementary Figs. 3, 4), similar to previous findings[32]. Carbon fixation rates increased from the colony center to its periphery (Fig. 3e, g), suggesting that carbon fixation was limited by DIC diffusion in the colony center (Fig. 4g–j and Supplementary Fig. 5a, c). The effects of OA on carbon fixation also exhibited spatial variation (Fig. 3e, g). OA lowered carbon fixation near the colony periphery (Fig. 3i), where the reduced pH mainly controlled by the environment (Fig. 4f) intensively inhibited photosynthetic energy production. Conversely, OA elevated carbon fixation near the colony center (Fig. 3i). This was because the high photosynthesis there consumed most $CO_2$, resulting in elevated pH levels inside the colony (Fig. 4f, k), thus diminishing the negative OA effects. Meanwhile, OA also resulted in a compensation of DIC limitation for carbon fixation mainly in the form of $HCO_3^-$ (Fig. 4l).

During the subsequent light period (3−12 h) when the carbon fixation rates were low to moderate (Fig. 3e, g), OA slightly reduced carbon fixation (Fig. 3i). This decline was mainly attributed to reduced photosynthetic

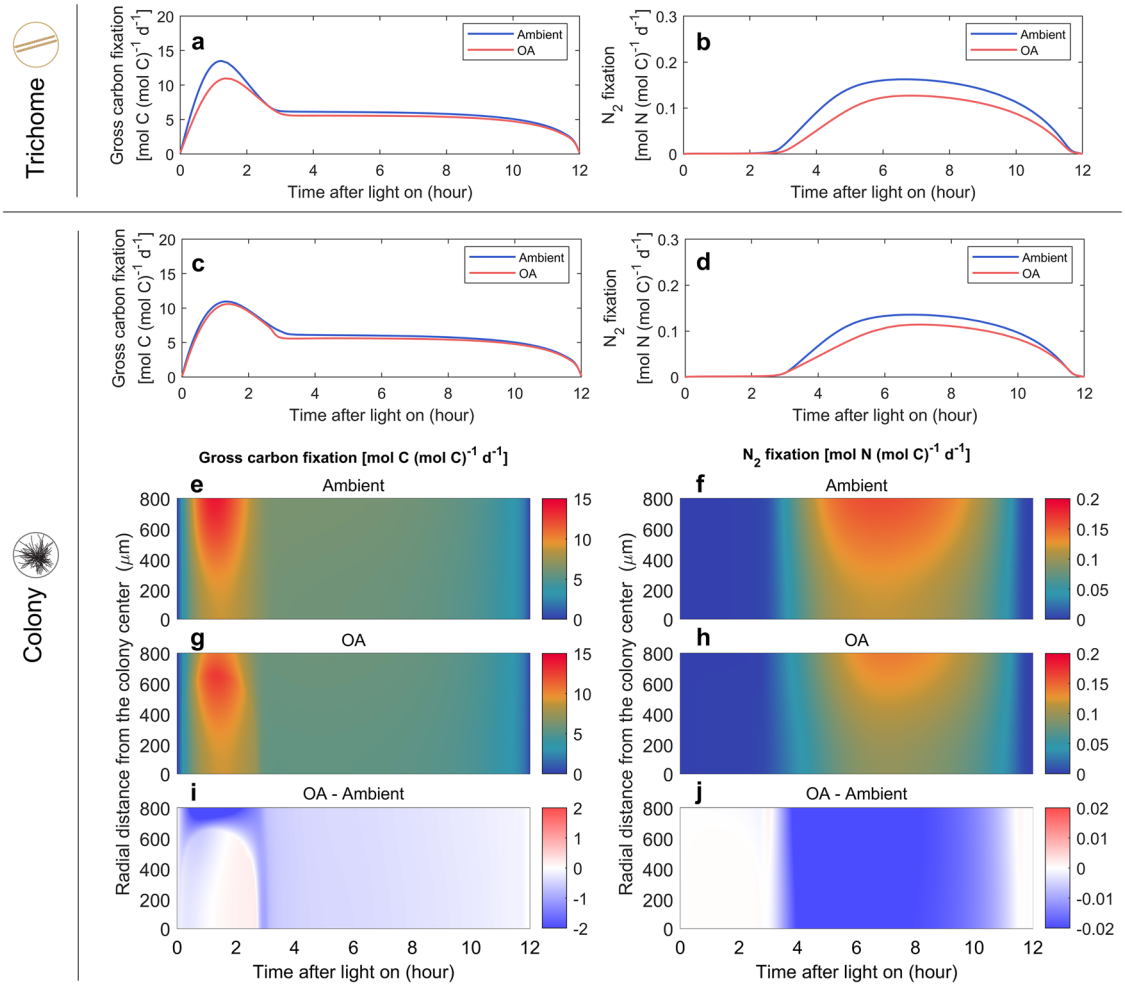


**Fig. 3 | Model results of *Trichodesmium* trichome and colony under limiting Fe condition. a**, **b** The comparison of the trichome model results under ambient and acidified (OA) conditions. The colony model results under ambient and OA conditions are compared in both (**c**, **d**) their average temporal and (**e**–**j**) spatiotemporal patterns. The spatiotemporal results include those under ambient conditions (**e**, **f**), OA conditions (**g**, **h**) and OA minus ambient results (**i**, **j**). Left panels present gross carbon fixation rates and right panels are $N_2$ fixation rates. The simulation was under a limiting Fe′ concentration of 40 pM. The sketch of *Trichodesmium* colony was modified from Klawonn et al. [36].

efficiency associated with lowered pH in the colony microenvironment (Fig. 4f).

We then analyzed $N_2$ fixation within the modeled colony, which, similar to the modeled trichome, primarily occurred from the middle to the late light period (Fig. 3f, h). During this period, there was a net consumption of microenvironmental $O_2$ driven by respiration (Supplementary Fig. 5) in order to help maintain low intracellular $O_2$. Consequently, $CO_2$ production and the associated pH reduction were more pronounced in the denser colony center (Fig. 4b, d). This localized acidification lowered nitrogenase efficiency more strongly in the colony center, forming a spatial gradient of declining $N_2$ fixation rates from the periphery to the center under both ambient and acidified conditions (Fig. 3f, h).

When comparing acidified to ambient conditions, OA further inhibited the $N_2$ fixation rate, with the magnitude of decrease being relatively uniform across the entire colony (Fig. 3j).

The simulation of *Trichodesmium* colony under Fe repletion resulted in similar patterns of carbon and $N_2$ fixation (Supplementary Figs. 1 and 6) and chemical gradients in the microenvironment (Supplementary Fig. 7).

## A brief summary

In this study, we constructed models to systematically examine the response of the globally important $N_2$-fixing cyanobacteria *Trichodesmium* to OA. Our analysis focused on comparing the responses of two major morphotypes: free trichomes and colonies. A series of previously reported findings on OA effects on *Trichodesmium* were integrated into the models. We used our models to address the conflicting observations that OA impaired growth and $N_2$ fixation rates of *Trichodesmium* free trichomes while it did not substantially impact or even enhanced those of *Trichodesmium* colonies[28–31].

## Impacts of OA on free *Trichodesmium* trichomes

Our free trichome model successfully simulated negative impact of OA. A previous study investigated the OA effects on *Trichodesmium* trichomes using a steady-state model[26]. In the present study, including diurnally dynamic simulations of various intracellular processes did not change the major conclusions from the steady-state model: The positive effects of OA, resulting from CCM energy savings, were outweighed by its negative effects, including reduced nitrogenase efficiency and downregulated ATP production (Fig. 5 and Supplementary Table 2). This was despite the compensation for reduced nitrogenase efficiency through an increased allocation of Fe to nitrogenase. Nevertheless, comparing to the steady-state model[26], the present model revealed some interesting diurnal dynamics. First, OA led to a reduction in energy (ATP) expenditure on CCM by about 1% as reported in the steady-state model[26] (Supplementary Table 2). Overall, in our model, the CCM energy-saving effect played a limited role in regulating the OA effects on free trichomes (Fig. 5a).

Second, OA inhibited nitrogenase efficiency and lowered $N_2$ fixation rates (Fig. 5c), particularly during the mid to late light period when $N_2$ fixation activity was high (Fig. 3b). Meanwhile, OA led to increased

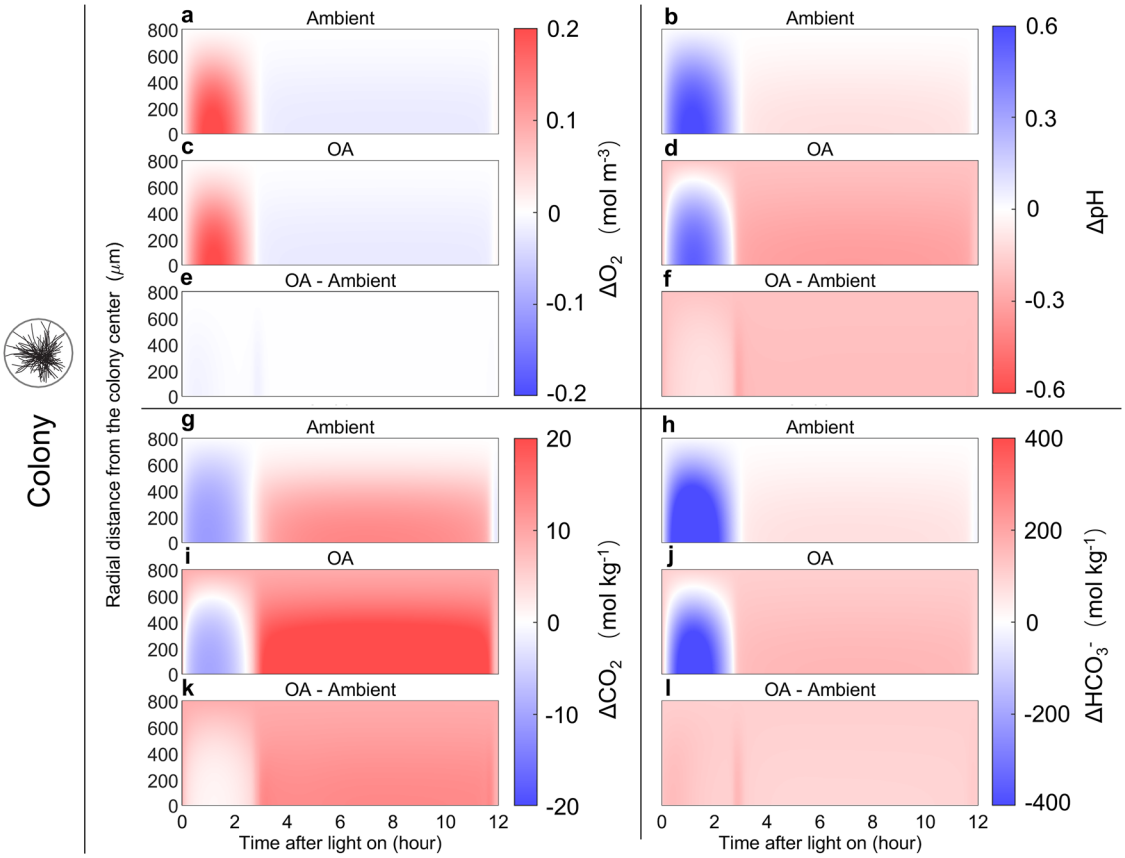


**Fig. 4 | Simulated $O_2$, pH, $CO_2$ and $HCO_3^-$ concentrations in the microenvironment of the colony under limiting Fe. a**, **c**, **e** $O_2$ concentrations. **b**, **d**, **f** pH values. **g**, **i**, **k** $CO_2$ concentrations. **h**, **j**, **l** $HCO_3^-$ concentrations. The colony models were simulated under ambient (**a**, **b**, **g**, **h**) or OA (**c**, **d**, **i**, **j**) conditions with Fe′ concentration of 40 pM. The concentrations of these parameters are shown as anomaly to ambient far-field conditions. The changes of these concentrations caused by OA are also displayed (**e**, **f**, **k**, **l**). To ensure consistency with Figs. 2 and 6, the color scale for pH is intentionally defined such that red denotes lower values (e.g., acidic pH) and blue denotes higher values (e.g., alkaline pH).

allocation of Fe to nitrogenase as a compensatory mechanism to counter its reduced efficiency (Fig. 5e). This was observed in a study conducting diurnal measurements of the Fe quota of nitrogenase[23]. The pH inhibition effect on nitrogenase outweighed the positive compensation from elevated Fe allocation to nitrogenase (Supplementary Fig. 8a)[2,23,26].

Third, OA impaired the thylakoid proton gradient, likely by requiring increased proton pumping to offset a lowered cytosolic pH[2]. This in turn inhibited ATP production via PET and reduced maximal $N_2$ fixation potential, particularly during the period with active $N_2$ fixation (Fig. 5g). This effect reduced $N_2$ fixation by approximately 10%, consistent with the early daily-averaged modeling[26]. Although *Trichodesmium* partly compensated reduction in ATP production by increasing the fraction of AET, this came at the cost of decreased NADPH production from LPET (Supplementary Fig. 9), aligning with previous findings[24].

Fourth, our model results indicated that OA could delay the formation of the low intracellular $O_2$ window (Supplementary Fig. 2), partially accounting for the decrease in $N_2$ fixation (Fig. 5i). This delay was attributed to OA reducing ATP production and lowering carbon fixation by about 20% (Fig. 3a). Consequently, the reduced carbohydrate storage limited later respiratory protection, which was essential for creating the low-$O_2$ window (Supplementary Fig. 2).

### Impacts of OA on *Trichodesmium* colonies

Our colony model was currently unable to reproduce the observed neutral or positive OA effects on *Trichodesmium* colonies by solely simulating the same intracellular processes as the trichome model within the colony's microenvironmental dynamics of $O_2$ and carbonate system (Fig. 1). However, it did result in a less pronounced negative OA effect on *Trichodesmium* colony compared to the trichome (Fig. 2 and Supplementary Table 1). We then explored the model results to understand why the formation of *Trichodesmium* colonies could partly weaken the negative OA effects.

By comparing all OA effects on the $N_2$ fixation of *Trichodesmium* free trichomes and colonies (Fig. 5), the main difference was observed in how OA regulated the inhibition of intracellular $O_2$ on $N_2$ fixation. OA intensified the $O_2$ inhibition on the $N_2$ fixation of *Trichodesmium* free trichomes (Fig. 5i), but weakened this inhibition on *Trichodesmium* colonies (Fig. 5j). This is because OA partially alleviated the DIC limitation in *Trichodesmium* colonies and diminished the inhibition effects of OA on photosynthetic energy production during the early light period. Consequently, unlike free *Trichodesmium* trichomes, where the formation of the low-$O_2$ window was delayed under OA (Supplementary Fig. 2), carbohydrate synthesis and storage in *Trichodesmium* colonies in the early light period were enhanced by OA (Fig. 3i). Furthermore, the increased microenvironmental $CO_2$ availability especially during the middle daytime (Fig. 3g, i) can modulate the activity of CCM, reducing the energy cost associated with active $HCO_3^-$ transport and thereby supporting higher net energy investment in carbon fixation[40]. These two effects ensured a sufficient supply of organic carbon for respiratory protection and facilitating the formation and maintenance of the low-$O_2$ window required for $N_2$ fixation (Figs. 4e and 5j).

In addition to the respiratory effects, the colonial structure confers another advantage by modifying $O_2$ gradients, including efficient $O_2$ drawdown in the colony center during the low-$O_2$-window. The microenvironmental $O_2$ levels under OA conditions were however, not

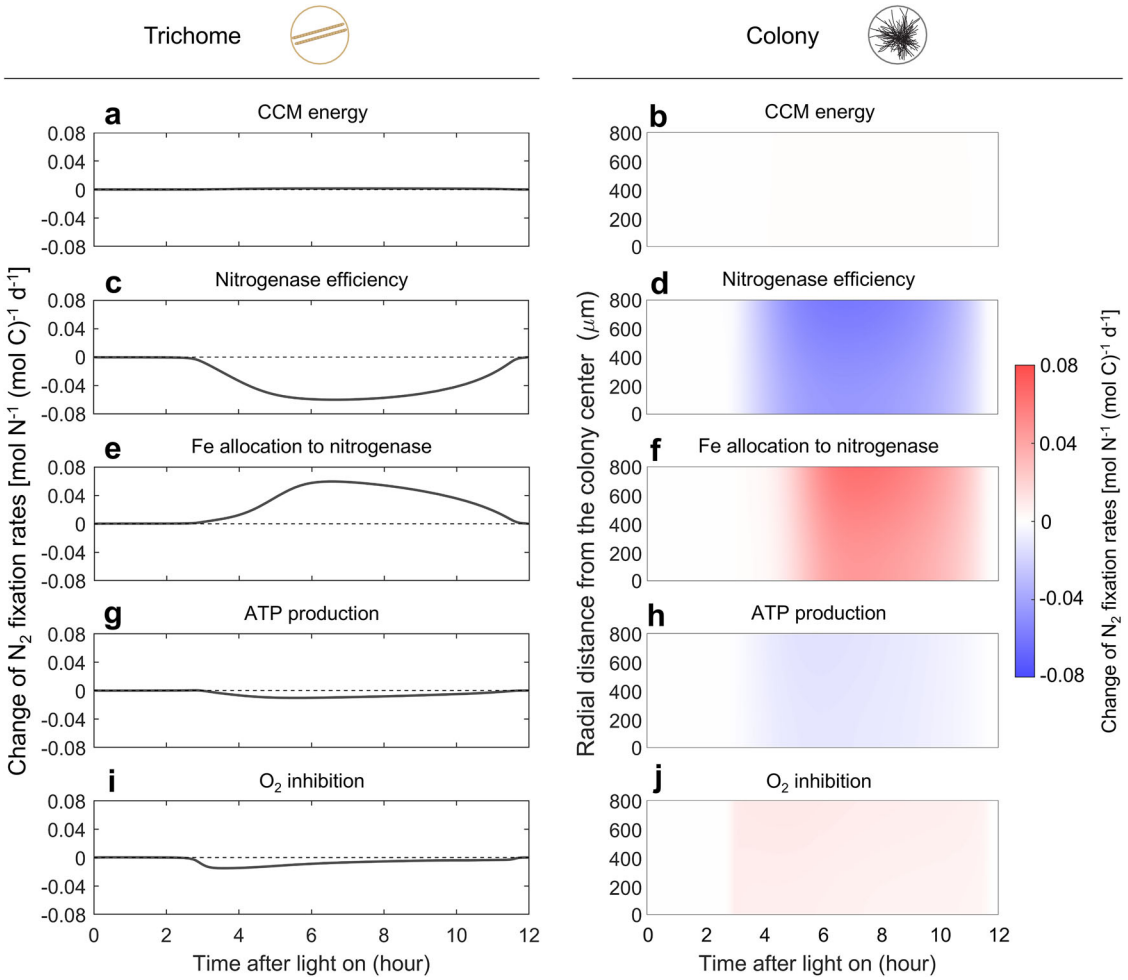


**Fig. 5 | Changes of $N_2$ fixation rates caused by each individual physiological effect of ocean acidification under Fe limitation.** The trichome (**left column**) and colony (**right column**) models were simulated under ambient or acidified (OA) conditions with Fe limitation (Fe′ = 40 pM). Each OA effect is calculated as the changes in $N_2$ fixation rates under OA conditions compared to ambient conditions, with only that specific effect implemented in the model. The shown OA effects include those on (**a**, **b**) energy savings by CCM, (**c**, **d**) the effect of pH on nitrogenase efficiency, (**e**, **f**) allocation of Fe to active nitrogenase, (**g, h**) inhibition of ATP production, and (**i**, **j**) the inhibition of $N_2$ fixation by intracellular $O_2$.

substantially different from those under ambient conditions (Fig. 4a, c). Therefore, the differences of colonies' response to OA from trichomes are not primarily attributed to altering $O_2$ diffusion gradients.

### Other potential positive OA effects on *Trichodesmium* colonies

Nevertheless, the mechanisms described above only slightly mitigated the negative effects of OA in the modeled *Trichodesmium* colony, while the reduced nitrogenase efficiency still dominated the overall OA effect (Fig. 5d). Hence, the models failed to reproduce the previously observed neutral or positive responses to OA, although it had incorporated known and reasonably expected mechanisms. Meanwhile, the simulated chemical gradients and their diurnal variations in the colony's microenvironment closely aligned with observations, including an approximately 200% supersaturated $O_2$ level and elevated pH during the early light period, followed by a decline in both $O_2$ and possibly pH at midday in the center of *Trichodesmium* colonies[30,41]. We therefore explored other mechanisms not yet represented in our model that could potentially benefit *Trichodesmium* colonies in response to OA.

OA may promote the Fe acquisition of *Trichodesmium* colonies. Studies have shown that *Trichodesmium* colonies can accumulate Fe-rich dust at their center[15]. Furthermore, it has been observed that OA can facilitate the ligand-promoted dissolution of these Fe-rich minerals in *Trichodesmium* colonies by approximately 10% for a decrease of 0.2 in pH[15,42,43]. Additionally, OA can increase $H_2$ evolution by more than 30% in *Trichodesmium*[23]. It has been observed that $H_2$ can promote the uptake of Fe in *Trichodesmium* colonies, hypothetically because $H_2$ acts as an electron source for reductive Fe dissolution[44]. As probably only a small portion of Fe dissolution uses $H_2$ as the electron source, this $H_2$-mediated increase in Fe dissolution could be substantially lower than 30%, the observed increasing rate of $H_2$ evolution under OA. Nevertheless, this line of evidence suggests another possible mechanism that OA can enhance Fe acquisition in *Trichodesmium* colonies and promote their $N_2$ fixation and growth.

To study the potential of this mechanism, we conducted model experiments by increasing intracellular metabolic Fe in *Trichodesmium* colony under OA (Fig. 6a). The results demonstrated that the overall OA effect on *Trichodesmium* growth could shift from negative to positive when the metabolic Fe in the modeled colony increased by 40% in the limiting-Fe conditions (Fig. 6a) and by 60% in the replete-Fe conditions (Supplementary Fig. 10c). These required Fe increases, based on the discussion above, are unlikely satisfied solely by ligand-promoted and/or $H_2$-mediated Fe acquisition. While the magnitude of OA-effects on Fe dissolution remains poorly understood, it is noteworthy that some field observations from areas with higher dust deposition, where *Trichodesmium* may rely more on dust-derived iron, have revealed stronger positive OA responses. For example, OA substantially increased $N_2$ fixation of *Trichodesmium* colonies in the Gulf of Mexico[31], where dust deposition events were frequent and heavy[45]. In

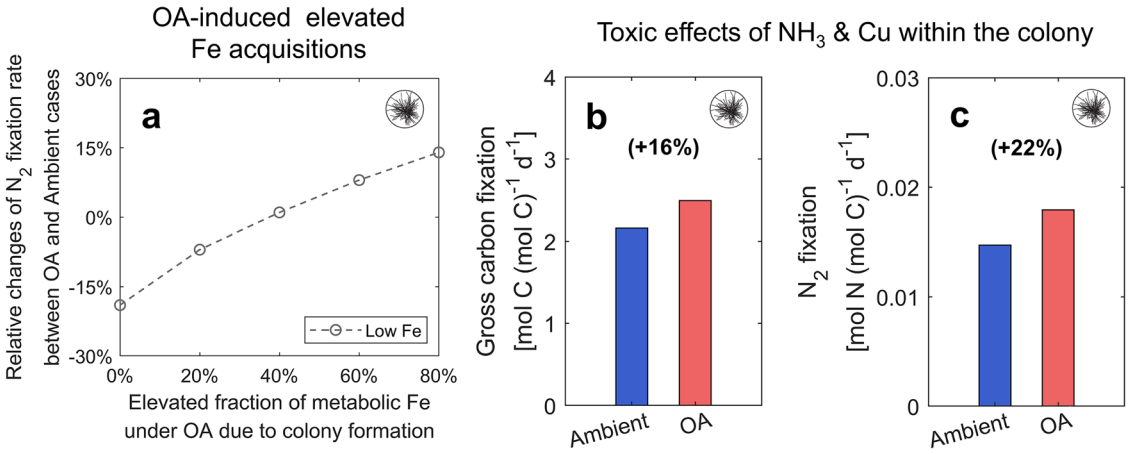


**Fig. 6 | Model results of other potential OA effects on Fe-limited *Trichodesmium* colonies. a** Changes in colony $N_2$ fixation rates under OA relative to ambient conditions, highlighting the potential benefit of OA-induced Fe acquisition enhancement. **b**, **c** Effects of modeled ammonia ($NH_3$) and copper (Cu) toxicity on carbon and $N_2$ fixation rates (normalized to carbon biomass). Microenvironmental ammonium ($NH_4^+$) decreases from 1.0 μmol $L^{-1}$ in the colony center to 0.4 μmol $L^{-1}$ at the periphery, based on Klawonn et al. [36].; microenvironmental $NH_3$ concentration is derived from the $NH_4^+$ concentration, modeled pH, and the $NH_3/NH_4^+$ equilibrium constant. The microenvironmental Cu follows the same spatial patterns as $NH_4^+$, with a maximum of 1 nmol $L^{-1}$ in the center[47]. All colony simulations were conducted under a limiting Fe′ level (40 pM)[23].

contrast, the OA effect on *Trichodesmium* colonies was insignificant in the North Pacific subtropical gyre[28], where dust deposition was relatively scarce and light[46].

Additionally, OA may benefit *Trichodesmium* colonies by reducing the toxicity of copper (Cu) and ammonia ($NH_3$). Copper released from concentrated dust particles inside *Trichodesmium* colonies can accumulate in the colony's microenvironment. Based on previous observations[47], we estimated that the Cu in the colony's microenvironment could reach concentrations higher than 1 nmol $L^{-1}$ (see "Supplementary Note 1"). Concurrently, symbiotic microorganisms inhabiting the microenvironment of *Trichodesmium* colonies can drive various nitrogen transformations, which, together with ammonium ($NH_4^+$) release by *Trichodesmium*, leading to $NH_4^+$ concentrations reaching as high as 1 μmol $L^{-1}$[36]. These naturally occurring levels of Cu and $NH_3$ have been found to be toxic to free *Trichodesmium* trichomes in laboratory experiments, where *Trichodesmium* was cultured in YBC-II media containing 1 nmol $L^{-1}$ Cu and 1 μmol $L^{-1}$ $NH_4^+$[2,48]. These studies also suggest that the increased $H^+$ concentration under OA can reduce Cu and $NH_3$ concentrations by downregulating their complexation with $CO_3^{2-}$ and $OH^-$[49], thereby promoting growth and $N_2$ fixation in *Trichodesmium*. Although these experiments were conducted with free *Trichodesmium* trichomes, the mechanisms may also apply to *Trichodesmium* colonies, given the similar Cu and $NH_4^+$ concentrations in the microenvironment of the colonies and in the media used to culture the free trichomes.

To reproduce the interactions between OA effects and these contaminations, we set up model experiments for *Trichodesmium* colonies. These experiments assumed that Cu and/or $NH_3$ toxicity could inhibit photosynthetic ATP production via PET[2,50], while OA might partially mitigate this inhibitory effect (see "Methods"). The model results showed that the toxicity could shift the responses of modeled colony to OA from negative to positive (Fig. 6b, c, Supplementary Fig. 11 and Supplementary Table 3). In the presence of Cu and $NH_3$ toxicity, OA not only enhanced $N_2$ fixation potential of *Trichodesmium* colonies but also increased their carbon fixation rates (Fig. 6b and Supplementary Fig. 11). This led to greater carbohydrate accumulation during the early light period (Supplementary Fig. 11), which facilitated the formation of the low-$O_2$ window (Supplementary Fig. 11), further promoting $N_2$ fixation rates (Fig. 6c and Supplementary Fig. 11). While the results certainly depended on the degree of the toxic effects simulated in the model, the model experiments suggest a hypothetical mechanism for explaining the observed positive responses of $N_2$ fixation in *Trichodesmium* colonies to OA. Furthermore, after incorporating elevated Fe acquisition into the toxicity testing experiments, the positive effects of OA on colonies became more pronounced (Supplementary Fig. 12).

### Broader context: Model-revealed mechanisms for lowered growth when *Trichodesmium* trichomes form colonies

In both laboratory experiments and in situ investigations, *Trichodesmium* colonies often exhibit lower $N_2$ fixation than *Trichodesmium* trichomes[41,51,52]. Various mechanisms for this phenomenon have been proposed, including increased photorespiration and $CO_2$ limitation of carbon fixation in the colonies[32,41]. Our model prediction coincides with these results. Here, based on our model results, we also propose other mechanisms in a viewpoint of the diurnal dynamics in the microenvironment of *Trichodesmium* colonies.

First, the low pH levels in the microenvironment of *Trichodesmium* colonies during the low-$O_2$, high $N_2$ fixation period (approximately 3–11 h) (Fig. 4b) reduce the nitrogenase efficiency. Second, during the early light period, the low DIC concentrations in *Trichodesmium* colony microenvironment limit their carbon fixation (Fig. 4g, h and Supplementary Table 1). Third, due to accumulated $O_2$ in the *Trichodesmium* colony microenvironment during the early light period (Fig. 4a), the colonies have to allocate a higher proportion of fixed carbon to respiratory protection when forming the low-$O_2$ environment necessary for $N_2$ fixation in later light period (Supplementary Table 1), which thereby reduces the organic carbon available for biosynthesis (Supplementary Table 1). Fourth, the toxic effects from $NH_3$ and/or Cu in *Trichodesmium* colonies can also account for the lowered $N_2$ fixation and growth (Supplementary Tables 1 and 3).

In addition, it has been proposed that the elevated photorespiration in *Trichodesmium* colonies can partially contribute to reduce $N_2$ fixation and growth[41]. The hypothesis is that high $O_2$ and low $CO_2$ concentrations in colony's microenvironment can stimulate photorespiration catalyzed by ribulose bisphosphate carboxylase oxygenase (RubisCO)[41,53,54] and reduce photosynthetic energy production and carbon fixation. Although our model did not incorporate this mechanism, the results supported the hypothesis by simulating the colony microenvironment, which featured supersaturated $O_2$ levels but limited $CO_2$ conditions during the early light period when photosynthesis activity was high (Fig. 4).

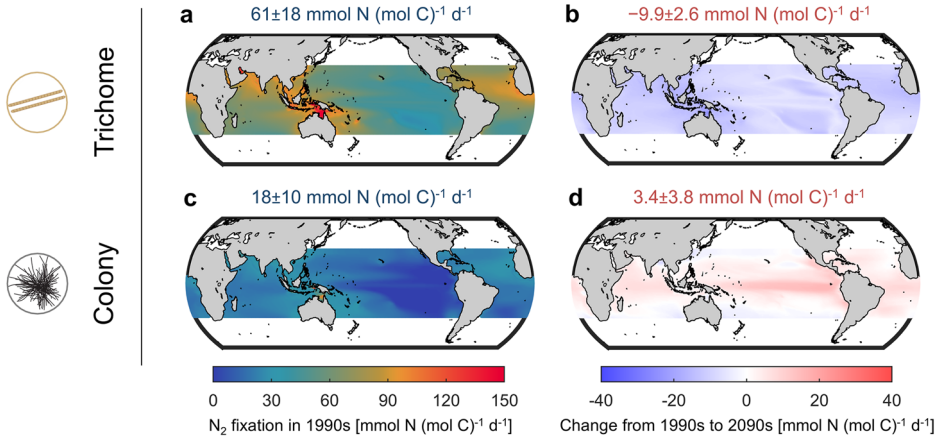


**Fig. 7 | The projected biomass-specific $N_2$ fixation rate of *Trichodesmium* trichome and colony.** **a**, **c** Results in 1990s. **b**, **d** Change from 1990s to 2090 s.

### Broader implications: Global projection of responses of *Trichodesmium* trichomes and colonies to OA

Using global-scale carbonate system parameters from an Earth system model (CESM-BGC) as inputs (see "Methods"), our model projected that the biomass-specific $N_2$ fixation rates of *Trichodesmium* trichomes averaged 61 ± 18 (mean ± s.d.) mmol N (mol C)$^{-1}$ d$^{-1}$ in the global ocean during the 1990s (Fig. 7a). High rates were projected in the Indonesian archipelago and northern Australian seawaters, and low rates were found in the eastern subtropical South and North Pacific (Fig. 7a). This spatial heterogeneity is consistent with both observational[8,11,55] and modeling studies[25,26,56]. Under the Representative Concentration Pathway (RCP) 4.5 intermediate climate scenario, biomass-specific $N_2$ fixation rates of the trichomes are projected to decline by 16 ± 6.4% from the 1990s to the 2090 s (Fig. 7b).

Our model projected lower biomass-specific $N_2$ fixation rates for *Trichodesmium* colonies during the 1990s [18 ± 10 mmol N (mol C)$^{-1}$ d$^{-1}$] (Fig. 7c), despite exhibiting a spatial distribution similar to that of the trichomes (Fig. 7a). In contrast, under RCP4.5, colonies were projected to increase their $N_2$ fixation rates in most tropical and subtropical oceans by 19 ± 24% by the 2090 s, markedly different from the decline projected for trichomes (Fig. 7). This suggests that colonies may adapt more effectively and exhibit greater resilience than free trichomes to future acidifying oceans. Regionally, increases in $N_2$ fixation rates of colonies prevailed especially in equatorial oceans and Atlantic subtropical gyres, where the dissolved inorganic Fe concentrations were generally high (>100 pM in surface waters)[57,58]. Specifically, our projections captured previous observations for *Trichodesmium* colonies, including positive OA effects on $N_2$ fixation in the Gulf of Mexico and at the station of Bermuda Atlantic Time-series Study (BATS)[29,31] and neutral or positive responses near Station ALOHA[28,30].

The total $N_2$ fixed by trichomes and colonies was subsequently estimated by scaling their respective biomass concentrations. Critically, while the global biomass distributions of both *Trichodesmium* trichomes and colonies remain poorly constrained (Supplementary Fig. 13)[55], incorporating their mean observed biomass concentrations (trichomes: $10^{1.1\pm1.6}$ µmol C L$^{-1}$; colonies: $10^{1.6\pm1.8}$ µmol C L$^{-1}$) (Supplementary Fig. 13) revealed opposing trends in global $N_2$ fixation between the two morphotypes from the 1990s to the 2090 s. Trichomes exhibited a decline of −8.1 Tg N yr$^{-1}$, whereas colonies increased by +8.5 Tg N yr$^{-1}$. Therefore, despite the considerable associated uncertainty, accounting for colony $N_2$ fixation demonstrably mitigates the overestimation of negative OA impacts that arises from considering only trichomes, as in most previous studies. Moreover, when both morphotypes are included, the model projected a slight net global increase in *Trichodesmium* $N_2$ fixation (+0.43 Tg N yr$^{-1}$), suggesting an overall near-neutral effect of OA on this key biogeochemical process. To improve the reliability of such assessments, future work should aim to simultaneously simulate the biomass dynamics of both *Trichodesmium* trichomes and colonies, along with their differential responses to acidification, within marine biogeochemical models.

### Limitations and future directions

This model study of *Trichodesmium* trichomes and colonies has several limitations. First, due to insufficient empirical data, the model did not account for phosphorus limitation[59] which is known to amplify the responses of *Trichodesmium* to OA[25]. Future work will aim to incorporate phosphorus limitation as more data on dynamic cellular phosphorus allocation under OA becomes available. Furthermore, the model did not include potential synergistic effects from other environmental variables, such as temperature[60].

Second, the model did not simulate the diverse microbiome associated with *Trichodesmium* colonies, which contributes to the uptake of organic phosphate via quorum sensing[61] and to the utilization of dust-derived iron through the production of Fe-chelating siderophores[62–64]. Additionally, interactive metabolic plasticity regulation with *Trichodesmium*[16], such as specific affinities for $CO_2$, may help combat the stress induced by OA[28].

Third, the model did not account for reactive oxygen species (ROS) generation and scavenging. Under high light and elevated $CO_2$, disruptions in PET can enhance ROS production, posing oxidative stress that may damage cellular components and reduce photosynthetic efficiency. *Trichodesmium* can counter this through an array of defense mechanisms, including not only enzymatic detoxification by superoxide dismutase and ascorbate peroxidase as well as Mehler-like reaction catalyzed by flavoproteins[65,66], but also non-enzymatic antioxidants such as carotenoids[67], and protective proteins (e.g., IdiA or IsiA) expressed under oxidative stress, especially when iron is limiting[68–70].

Fourth, the model did not include physiological acclimation mechanisms, such as enhanced proton pumping, altered electron transport, upregulated Mehler reaction activity, or broader proteome restructuring[53,59]. Such acclimation responses could mitigate low-pH stress on carbon fixation and may account for discrepancies with long-term experiments (e.g., >3 months) that report $CO_2$-induced stimulation of $N_2$ fixation under moderate light conditions[53,59,71–73]. Our model, which is parameterized based on pre-acclimation physiological constraints, does not reproduce this stimulation under either low or high light intensities (Supplementary Fig. 14). This represents a key direction for future development, especially considering that seawater carbonate chemistry varies over multiple timescales in nature, whereas laboratory experiments typically apply sudden changes rather than gradual transitions, and then maintain steady-state acidified conditions. Thus, responses observed under controlled experimental settings may underestimate the acclimation capacity of *Trichodesmium* in the real-world environment.

Last, this model did not consider another common morphology of *Trichodesmium*, the tuft-shaped colonies, which have been found to respond more positively to OA than puff-shaped *Trichodesmium* colonies[28]. Whether this phenomenon is common and what causes it is still unknown.

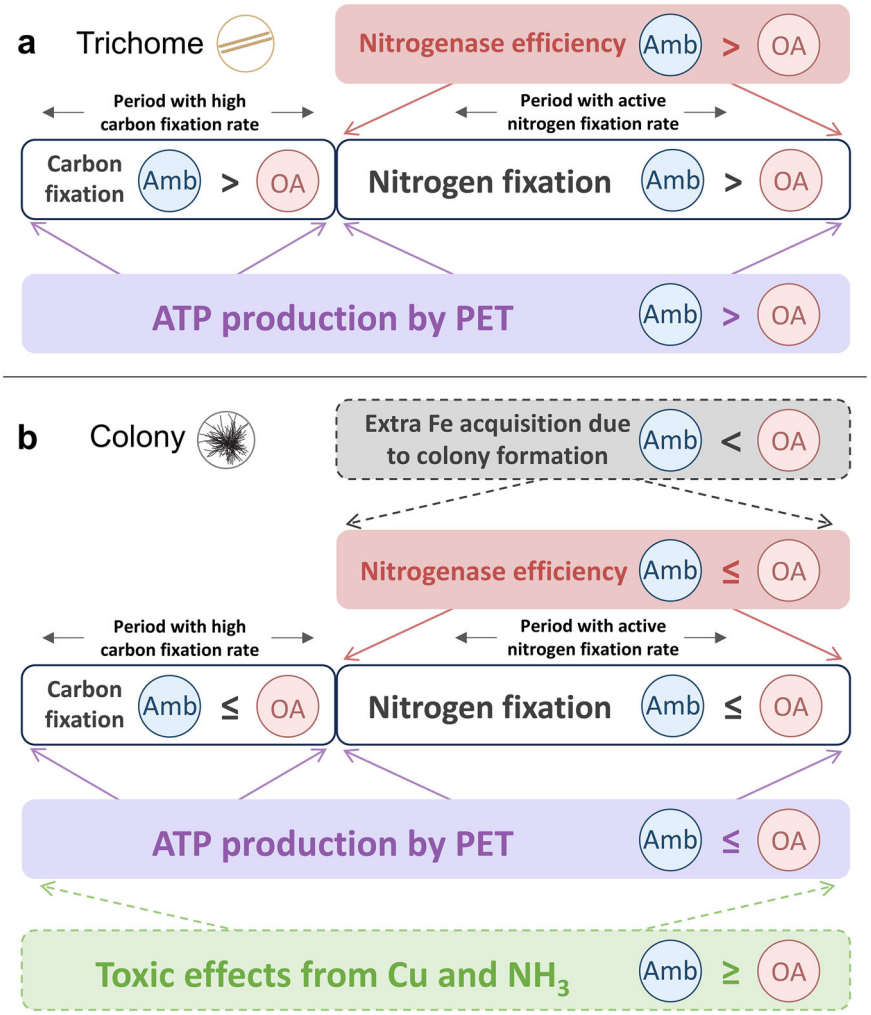


**Fig. 8 | Schematic diagram of the response of *Trichodesmium* to ocean acidification. a** The response of trichomes to ocean acidification. **b** The response of colonies to ocean acidification. PET photosynthetic electron transfer, Amb ambient condition, OA acidified condition. The dash-edged bars and dashed arrows represent hypothetical mechanisms and effects.

## Conclusions

In summary, this study provides a mechanistic understanding of how OA impacts $N_2$ fixation and growth differently in *Trichodesmium* trichomes and colonies. By resolving the diurnal and spatial dynamics of *Trichodesmium*'s physiological processes and the chemical properties of their microenvironment, the models have revealed mechanisms that were either previously unknown or inadequately explained. In *Trichodesmium* trichomes, the decline in $N_2$ fixation and growth rates under OA is primarily attributed to decreased nitrogenase efficiency and reduced energy production (Fig. 8a). In contrast, in *Trichodesmium* colonies, mechanisms such as enhanced Fe acquisition and the mitigation of naturally occurring Cu and $NH_3$ toxicity within the colony's microenvironment enable a shift from negative to positive responses to OA (Fig. 8b). This underscores the critical role of chemical gradients at the microenvironmental scale in regulating $N_2$ fixation within *Trichodesmium* colonies. Furthermore, the study's findings on the diurnal variations in OA's impact on $N_2$ fixation emphasize the need for high-temporal-resolution observations to gain deeper insights into the mechanisms through which OA regulates $N_2$ fixation in *Trichodesmium*. By 2090s, global projections under RCP4.5 demonstrate $N_2$ fixation decline in trichomes but increase in colonies, indicating colonies' resilience and plasticity in acidifying future oceans. Our mechanistic study synergistically connects physiological factors governing metabolic rates in *Trichodesmium* colonies versus free trichomes, providing a framework essential for a realistic prediction of how this globally important microbe may respond to a changing environment.

## Methods

In the following, we briefly describe the model schemes. For the details of the models, including parameter values and variables, refer to the Supplementary Note 1 and Supplementary Tables 4–7.

The model framework for *Trichodesmium* integrates physiological processes across cellular and microenvironmental scales, capturing the dynamics of both free trichomes and colonies under OA. The trichome model simulates key processes, including LPET, AET, CCM, carbon fixation, $N_2$ fixation, respiratory protection, and intracellular Fe allocation. ATP and NADPH produced by PET are allocated to these processes to constrain their rates, with Fe availability serving as an additional limiting factor. OA influences these dynamics by altering Fe allocation, impairing ATP production, modifying energy consumption in CCM, and reducing nitrogenase efficiency. The growth is co-limited by fixed carbon and nitrogen over the diurnal period. The colony model builds upon the trichome framework, simulating extracellular microenvironmental properties, such as gradients of $O_2$ and carbonate system components ($CO_2$, $HCO_3^-$, and pH), within a porous spherical structure. These gradients arise from biological activities, extracellular chemical reactions, and physical diffusion, which are modulated by spatially varying porosity within the colony. Additional model experiments incorporate the effects of microenvironmental stressors, such as $NH_3$ and Cu toxicity. Parameter values and initial conditions were derived from experimental observations and optimized to maximize growth efficiency and rates under diurnal light period.

### Photosynthetic pathways

The total PET rate is modulated by light intensity and increases with the amount of Fe allocated to photosystems. It can be inhibited by respiratory protection[35]. The total PET rate is fractionated to LPET and AET depending on the instantaneous ATP and NADPH requirements of physiological processes (Fig. 1a). Both LPET and AET produce ATP, with the rate being downregulated under OA[2]. LPET also produces NADPH, whose production rate is not directly impacted by OA because, unlike ATP production, it is not driven by the proton gradient between the lumen and stroma[74,75].

### $N_2$ fixation

The maximal potential of $N_2$ fixation rate is calculated based on the assumption that ATP and NADPH produced by PET completely sustain $N_2$ fixation[37]. The $N_2$ fixation rate is also regulated by the Fe quota in nitrogenase and inhibited by intracellular $O_2$. Under OA, the reduced pH levels lower the efficiency of nitrogenase[2,26].

### $CO_2$ concentrating mechanism

The energy consumption rate for CCM is calculated based on the requirement of $HCO_3^-$ for carbon fixation and the cost for per $HCO_3^-$ transportation[22,26,40].The elevation of $CO_2$ concentration under OA can lower the energy need for CCM by reducing the requirement for $HCO_3^-$[19,20,76,77], with the saved energy benefitting carbon and $N_2$ fixations[19,78].

### Carbon fixation

Carbon fixation requires both NADPH and ATP[79]. The carbon fixation rate is determined at every time step by assuming that the NADPH and ATP produced by PET are instantaneously and fully utilized by intracellular processes[37].

### Respiratory protection

Respiratory protection is an active process that consumes carbohydrates to lower intracellular $O_2$ level, thereby supporting $N_2$ fixation as an indirect carbon cost[80,81]. Its rate is elevated when the requirement of $N_2$ fixation and the intracellular $O_2$ concentration increase[37]. Excess reductant from respiratory protection may enter the electron transport chain and can be dissipated via the Mehler reaction through the plastoquinone pool[70].

### $O_2$ and $CO_2$ diffusion

The $O_2$ and $CO_2$ diffusion occurs between the intracellular cytoplasm and the extracellular environment, which is parameterized using the scheme in Staal et al. [82] and Luo et al. [37].

$CO_2$ concentration in the cytoplasm was not simulated but set zero based on the assumption that $CO_2$ in the cytoplasm was assumed to be quickly transferred into carboxysome or leak into extracellular environment.

### Intracellular Fe pools and translocation

The intracellular Fe in metabolism and storage are calculated from the total intracellular Fe using a previous scheme[26]. The Fe requirement for the synthesis of photosystems and nitrogenase is from the buffer pool[27].

OA seemingly does not affect the general diurnal patterns of both photosystems and nitrogenase but their initial levels at the beginning of the light period[23], predefined in our model using observations[23]. The differences in the absolute amount of photosystems and nitrogenase between ambient and acidified conditions[23] were represented in the optimized maximal Fe translocation rates of them (Supplementary Table 6), which ensured optimal intracellular Fe allocations to achieve the maximal growth rate[27].

### Colony model framework

The colony is modeled as a porous sphere (radius = 800 μm)[36]. To accurately represent microenvironment concentration profiles, we implemented spatially variable porosity which decreases from the periphery to the center of colony and modulates biological processes as well as physical diffusion rates and is able to capture the minor effects of biomass distribution in the colony on chemical gradients (Supplementary Figs. 4 and 5). The porosity is calculated as the ratio of the non-biological volume to the sum of non-biological and biological volumes, using the scheme in Klawonn et al. [36].

Biological processes within the colony are parameterized similar to those in the free trichome model described above. Considering that there might be DIC limitation for carbon fixation of colony, especially at the center, we introduced the DIC limitation effect into the colony model. This effect is regulated by the concentration of $CO_2$ and $HCO_3^-$ in the microenvironment of colony, of which especially in the center $CO_2$ and $HCO_3^-$ concentrations could be low[32].

In the non-biological microenvironment of the colony, concentrations of $O_2$, $CO_2$, $HCO_3^-$, $CO_3^{2-}$, $H^+$, and $OH^-$ are simulated within the radical distance (≤800 μm). These concentrations are controlled by the physical diffusion which is reduced by the decrease in the porosity in the colony center, extracellular chemical reactions of the carbonate system, and intracellular biological processes (e.g., net uptake or release). Therefore, their changing rates with time and radical distance can be represented using diffusion-reaction equations[83].

### Model experiments with $NH_3$ and Cu toxicity

Considering that $NH_3$ and Cu can inhibit photosystem II activity and photosynthetic ATP production[2,50], we hypothesized that $NH_3$ and/or Cu toxicity would negatively affect the ATP production by PET. This effect is regulated by extracellular $NH_3$ and dissolved inorganic Cu concentrations with pH levels. In our model, this regulation could lead to a downregulation in PET, for example, from 50% to 30% under ambient conditions and from 30% to 10% under acidified conditions, from the center to the periphery of the colony (see "Supplementary Note 1"). Note that model experiments were conducted in free trichomes at first, of which model results were constrained using observations with artificially introduced toxicity (Supplementary Figs. 15 and 16)[2,48].

### Model parameter values

Some fixed parameters (Supplementary Table 4) were obtained from previous studies, while others (Supplementary Table 5) were derived from our model experiments. The simulations were performed under a constant light intensity of 90 μmol $m^{-2}$ $s^{-1}$, a representative level for laboratory cultures of *Trichodesmium* that supports robust growth and aligns with the experimental conditions of the reference study[23]. Model outputs for growth rates (Supplementary Table 8) and diurnal Fe in photosystems and nitrogenase (Supplementary Fig. 17) were constrained by observations under both ambient and acidified conditions[23]. Fe allocations to photosystems and nitrogenase at the beginning of light period were adopted the observations from a laboratory culture study[23].

In both the trichome and colony models under diurnal dynamic light intensity, we optimized four key model parameters (Supplementary Table 5) relevant to respiratory protection and iron allocation to maximize growth efficiency (i.e., carbon and iron utilization) and growth rate of *Trichodesmium*, including the maximal respiratory protection rate, the maximal synthesis and decomposition rates of photosystems, and the maximal synthesis rate of nitrogenase[84]. The optimization was performed using the global optimizer MultiStart in MATLAB.

### Global projection of $N_2$ fixation rates of *Trichodesmium* trichome and colony

The parameters of carbonate system were derived from an Earth system model (CESM-BGC) RCP 4.5 simulations in both 1990s and 2090s (http://www.earthsystemgrid.org)[57]. The Fe quota of *Trichodesmium* was calculated following Luo, et al. [26], using projected surface inorganic Fe concentrations (Fe') from CESM-BGC simulations in 1990s. Due to large uncertainty in projected dust deposition in future oceans[85], changes in Fe′ between the 1990s and 2090 s were not incorporated[20]. The OA-induced additional Fe acquisition (Fig. 6a) was omitted because of high associated uncertainties. The OA-induced mitigation of ammonia and copper toxicity (Fig. 6b, c) was considered in the global projection of colonies' $N_2$ fixation.

All global projections (Fig. 7) were confined to tropical and subtropical oceans where *Trichodesmium* may occur[55].

To compute the changes in total annual fixed nitrogen from the 1990s to the 2090s by trichomes and colonies, respectively, we incorporated the projected biomass-specific $N_2$ fixation rates for both periods (Fig. 7) and geometric mean biomass estimates from observations (Supplementary Fig. 13).

### Reporting summary

Further information on research design is available in the Nature Portfolio Reporting Summary linked to this article.

## Quantification and statistical analysis

### Code, plotting, data visualization and statistical analysis

The code for *Trichodesmium* models, plotting, data visualization and statistical analysis in this study are nearly all performed via MATLAB, with the diagram of model structure (Figs. 1 and 8) plotted by Power Point of Microsoft Office.

## Data availability

The data are available on Zenodo (https://doi.org/10.5281/zenodo.17217462).

## Code availability

The code is available on Zenodo (https://doi.org/10.5281/zenodo.17217462).

Received: 7 October 2025; Accepted: 17 February 2026;
Published online: 23 February 2026

## References

1. Doney, S. C., Busch, D. S., Cooley, S. R. & Kroeker, K. J. The impacts of ocean acidification on marine ecosystems and reliant human communities. *Annu. Rev. Environ. Resour.* **45**, 83–112 (2020).
2. Hong, H. et al. The complex effects of ocean acidification on the prominent $N_2$-fixing cyanobacterium *Trichodesmium*. *Science* **356**, 527–531 (2017).
3. Wu, S. et al. A rise in ROS and EPS production: new insights into the *Trichodesmium erythraeum* response to ocean acidification. *J. Phycol.* **57**, 172–182 (2021).
4. Shi, Y. & Li, Y. Impacts of ocean acidification on physiology and ecology of marine invertebrates: a comprehensive review. *Aquat. Ecol.* **58**, 207–226 (2024).
5. Reynolds, S. E. et al. How widespread and important is $N_2$ fixation in the North Atlantic Ocean? *Glob. Biogeochem. Cycles* **21**, GB4015 (2007).
6. Capone, D. G., Zehr, J. P., Paerl, H. W., Bergman, B. & Carpenter, E. J. *Trichodesmium*, a globally significant marine cyanobacterium. *Science* **276**, 1221–1229 (1997).
7. Zehr, J. P. & Capone, D. G. Changing perspectives in marine nitrogen fixation. *Science* **368**, eaay9514 (2020).
8. Capone, D. G. et al. Nitrogen fixation by *Trichodesmium* spp.: An important source of new nitrogen to the tropical and subtropical North Atlantic Ocean. *Glob. Biogeochem. Cycles* **19**, GB2024 (2005).
9. Berman-Frank, I., Lundgren, P. & Falkowski, P. Nitrogen fixation and photosynthetic oxygen evolution in cyanobacteria. *Res. Microbiol.* **154**, 157–164 (2003).
10. Mahaffey, C., Michaels, A. F. & Capone, D. G. The conundrum of marine $N_2$ fixation. *Am. J. Sci.* **305**, 546–595 (2005).
11. Wrightson, L., Yang, N., Mahaffey, C., Hutchins, D. A. & Tagliabue, A. Integrating the impact of global change on the niche and physiology of marine nitrogen-fixing cyanobacteria. *Glob. Change Biol.* **28**, 7078–7093 (2022).
12. Tzubari, Y., Magnezi, L., Be'er, A. & Berman-Frank, I. Iron and phosphorus deprivation induce sociality in the marine bloom-forming cyanobacterium *Trichodesmium*. *ISME J.* **12**, 1682–1693 (2018).
13. Pfreundt, U. et al. Controlled motility in the cyanobacterium *Trichodesmium* regulates aggregate architecture. *Science* **380**, 830–835 (2023).
14. Eichner, M., Inomura, K., Pierella Karlusich, J. J. & Shaked, Y. Better together? Lessons on sociality from *Trichodesmium*. *Trends Microbiol.* **31**, 1072–1084 (2023).
15. Rubin, M., Berman-Frank, I. & Shaked, Y. Dust- and mineral-iron utilization by the marine dinitrogen-fixer *Trichodesmium*. *Nat. Geosci.* **4**, 529–534 (2011).
16. Held, N. A. et al. Dynamic diel proteome and daytime nitrogenase activity supports buoyancy in the cyanobacterium Trichodesmium. *Nat. Microbiol.* **7**, 300–311 (2022).
17. Conroy, B. J. et al. Mesozooplankton graze on cyanobacteria in the Amazon River plume and western tropical North Atlantic. *Front. Microbiol.* **8**, 1436 (2017).
18. Webb, E. A. et al. Importance of mobile genetic element immunity in numerically abundant *Trichodesmium* clades. *ISME Commun.* **3**, 15 (2023).
19. Hutchins, D. A. et al. $CO_2$ control of *Trichodesmium* $N_2$ fixation, photosynthesis, growth rates, and elemental ratios: implications for past, present, and future ocean biogeochemistry. *Limnol. Oceanogr.* **52**, 1293–1304 (2007).
20. Levitan, O. et al. Elevated $CO_2$ enhances nitrogen fixation and growth in the marine cyanobacterium *Trichodesmium*. *Glob. Change Biol.* **13**, 531–538 (2007).
21. Kranz, S. A. et al. Combined effects of $CO_2$ and light on the $N_2$-fixing cyanobacterium *Trichodesmium* IMS101: physiological responses. *Plant Physiol.* **154**, 334–345 (2010).
22. Eichner, M., Kranz, S. A. & Rost, B. Combined effects of different $CO_2$ levels and N sources on the diazotrophic cyanobacterium *Trichodesmium*. *Physiol. Plant.* **152**, 316–330 (2014).
23. Shi, D., Kranz, S. A., Kim, J. M. & Morel, F. M. Ocean acidification slows nitrogen fixation and growth in the dominant diazotroph *Trichodesmium* under low-iron conditions. *Proc. Natl. Acad. Sci. USA* **109**, 3094–3100 (2012).
24. Zhang, F. et al. Proteomic responses to ocean acidification of the marine diazotroph *Trichodesmium* under iron-replete and iron-limited conditions. *Photosynth. Res.* **142**, 17–34 (2019).
25. Zhang, F. et al. Phosphate limitation intensifies negative effects of ocean acidification on globally important nitrogen fixing cyanobacterium. *Nat. Commun.* **13**, 6730 (2022).
26. Luo, Y. W. et al. Reduced nitrogenase efficiency dominates response of the globally important nitrogen fixer *Trichodesmium* to ocean acidification. *Nat. Commun.* **10**, 1521 (2019).
27. Luo, W. & Luo, Y.-W. Diurnally dynamic iron allocation promotes $N_2$ fixation in marine dominant diazotroph *Trichodesmium*. *Comput. Struct. Biotechnol. J.* **21**, 3503–3512 (2023).
28. Gradoville, M. R., White, A. E., Böttjer, D., Church, M. J. & Letelier, R. M. Diversity trumps acidification: Lack of evidence for carbon dioxide enhancement of *Trichodesmium* community nitrogen or carbon fixation at Station ALOHA. *Limnol. Oceanogr.* **59**, 645–659 (2014).
29. Lomas, M. W. et al. Effect of ocean acidification on cyanobacteria in the subtropical North Atlantic. *Aquat. Microb. Ecol.* **66**, 211–222 (2012).
30. Eichner, M. J. et al. Chemical microenvironments and single-cell carbon and nitrogen uptake in field-collected colonies of *Trichodesmium* under different $pCO_2$. *ISME J.* **11**, 1305–1317 (2017).
31. Hutchins, D. A., Mulholland, M. R. & Fu, F. Nutrient cycles and marine microbes in a $CO_2$-enriched ocean. *Oceanography* **22**, 128–145 (2009).

32. Eichner, M., Wolf-Gladrow, D. & Ploug, H. Carbonate chemistry in the microenvironment within cyanobacterial aggregates under present-day and future $pCO_2$ levels. *Limnol. Oceanogr.* **67**, 203–218 (2021).
33. Berman-Frank, I., Cullen, J. T., Shaked, Y., Sherrell, R. M. & Falkowski, P. G. Iron availability, cellular iron quotas, and nitrogen fixation in *Trichodesmium*. *Limnol. Oceanogr.* **46**, 1249–1260 (2001).
34. Coles, V. J. & Hood, R. R. Modeling the impact of iron and phosphorus limitations on nitrogen fixation in the Atlantic Ocean. *Biogeosciences* **4**, 455–479 (2007).
35. Berman-Frank, I. et al. Segregation of nitrogen fixation and oxygenic photosynthesis in the marine cyanobacterium *Trichodesmium*. *Science* **294**, 1534–1537 (2001).
36. Klawonn, I. et al. Distinct nitrogen cycling and steep chemical gradients in *Trichodesmium* colonies. *ISME J.* **14**, 399–412 (2020).
37. Luo, W., Inomura, K., Zhang, H. & Luo, Y.-W. $N_2$ fixation in *Trichodesmium* does not require spatial segregation from photosynthesis. *mSystems* **7**, e00538–22 (2022).
38. Chakraborty, S. et al. Quantifying nitrogen fixation by heterotrophic bacteria in sinking marine particles. *Nat. Commun.* **12**, 4085 (2021).
39. Hania, A., Lopez-Adams, R., Prasil, O. & Eichner, M. Protection of nitrogenase from photosynthetic $O_2$ evolution in *Trichodesmium*: methodological pitfalls and advances over 30 years of research. *Photosynthetica* **61**, 58–72 (2023).
40. Raven, J. A., Beardall, J. & Giordano, M. Energy costs of carbon dioxide concentrating mechanisms in aquatic organisms. *Photosynth. Res.* **121**, 111–124 (2014).
41. Eichner, M. et al. $N_2$ fixation in free-floating filaments of *Trichodesmium* is higher than in transiently suboxic colony microenvironments. *N. Phytol.* **222**, 852–863 (2019).
42. Eichner, M., Basu, S., Wang, S., Beer, D. & Shaked, Y. Mineral iron dissolution in *Trichodesmium* colonies: The role of $O_2$ and pH microenvironments. *Limnol. Oceanogr.* **65**, 1149–1160 (2019).
43. Kessler, N., Kraemer, S. M., Shaked, Y. & Schenkeveld, W. Investigation of siderophore-promoted and reductive dissolution of dust in marine microenvironments such as *Trichodesmium* colonies. *Front. Mar. Sci.* **7**, 45 (2020).
44. Eichner, M., Basu, S., Gledhill, M., de Beer, D. & Shaked, Y. Hydrogen dynamics in *Trichodesmium* colonies and their potential role in mineral iron acquisition. *Front. Microbiol.* **10**, 1565 (2019).
45. Lenes, J. M., Prospero, J. M., Landing, W. M., Virmani, J. I. & Walsh, J. J. A model of Saharan dust deposition to the eastern Gulf of Mexico. *Mar. Chem.* **134-135**, 1–9 (2012).
46. Hayes, C. T. et al. Thorium isotopes tracing the iron cycle at the Hawaii Ocean Time-series Station ALOHA. *Geochim. Cosmochim. Acta* **169**, 1–16 (2015).
47. Wang, S. et al. Costs of dust collection by *Trichodesmium*: effect on buoyancy and toxic metal release. *J. Geophys. Res.* **129**, e2023JG007954 (2024).
48. Shi, D., Shen, R., Kranz, S. A., Morel, F. M. M. & Hong, H. Response to Comment on "The complex effects of ocean acidification on the prominent $N_2$-fixing cyanobacterium *Trichodesmium*. *Science* **357**, eaao0428 (2017).
49. Morel, F. M. & Hering, J. G. *Principles and Applications of Aquatic Chemistry* (Wiley Inter-Science, 1993).
50. Cid, A., Herrero, C., Torres, E. & Abalde, J. Copper toxicity on the marine microalga *Phaeodactylum tricornutum*: effects on photosynthesis and related parameters. *Aquat. Toxicol.* **31**, 165–174 (1995).
51. Orcutt, K. M., Lipschultz, F., Gundersen, K., Arimoto, R. & Gallon, J. R. A seasonal study of the significance of $N_2$ fixation by *Trichodesmium* spp. at the Bermuda Atlantic Time-series Study (BATS) site. *Deep Sea Res. Part II Top. Stud. Oceanogr.* **48**, 1583–1608 (2001).
52. Sohm, J. A., Subramaniam, A., Gunderson, T. E., Carpenter, E. J. & Capone, D. G. Nitrogen fixation by *Trichodesmium* spp. and unicellular diazotrophs in the North Pacific Subtropical Gyre. *J. Geophys. Res.* **116**, G03002 (2011).
53. Boatman, T. G., Davey, P. A., Lawson, T. & Geider, R. J. $CO_2$ modulation of the rates of photosynthesis and light-dependent $O_2$ consumption in *Trichodesmium*. *J. Exp. Bot.* **70**, 589–597 (2019).
54. Li, H. & Gao, K. Deoxygenation enhances photosynthetic performance and increases $N_2$ fixation in the marine cyanobacterium *Trichodesmium* under elevated $pCO_2$. *Front. Microbiol.* **14**, 1102909 (2023).
55. Shao, Z. et al. Global oceanic diazotroph database version 2 and elevated estimate of global oceanic $N_2$ fixation. *Earth Syst. Sci. Data* **15**, 3673–3709 (2023).
56. Boatman, T. G., Upton, G. J. G., Lawson, T. & Geider, R. J. Projected expansion of *Trichodesmium*'s geographical distribution and increase in growth potential in response to climate change. *Glob. Change Biol.* **26**, 6445–6456 (2020).
57. Moore, J. K., Lindsay, K., Doney, S. C., Long, M. C. & Misumi, K. Marine ecosystem dynamics and biogeochemical cycling in the Community Earth System Model [CESM1(BGC)]: comparison of the 1990s with the 2090s under the RCP4.5 and RCP8.5 scenarios. *J. Clim.* **26**, 9291–9312 (2013).
58. Knapp, A. N., Casciotti, K. L., Berelson, W. M., Prokopenko, M. G. & Capone, D. G. Low rates of nitrogen fixation in eastern tropical South Pacific surface waters. *Proc. Natl. Acad. Sci. USA* **113**, 4398–4403 (2016).
59. Walworth, N. G. et al. Mechanisms of increased *Trichodesmium* fitness under iron and phosphorus co-limitation in the present and future ocean. *Nat. Commun.* **7**, 12081 (2016).
60. Jiang, H.-B. et al. Ocean warming alleviates iron limitation of marine nitrogen fixation. *Nat. Clim. Change* **8**, 709–712 (2018).
61. Van Mooy, B. A. S. et al. Quorum sensing control of phosphorus acquisition in *Trichodesmium* consortia. *ISME J.* **6**, 422–429 (2012).
62. Frischkorn, K. R., Rouco, M., Van Mooy, B. A. S. & Dyhrman, S. T. Epibionts dominate metabolic functional potential of *Trichodesmium* colonies from the oligotrophic ocean. *ISME J.* **11**, 2090–2101 (2017).
63. Frischkorn, K. R., Haley, S. T. & Dyhrman, S. T. Coordinated gene expression between *Trichodesmium* and its microbiome over day-night cycles in the North Pacific Subtropical Gyre. *ISME J.* **12**, 997–1007 (2018).
64. Basu, S., Gledhill, M., de Beer, D., Prabhu Matondkar, S. G. & Shaked, Y. Colonies of marine cyanobacteria *Trichodesmium* interact with associated bacteria to acquire iron from dust. *Commun. Biol.* **2**, 284–284 (2019).
65. Allahverdiyeva, Y., Isojärvi, J., Zhang, P. & Aro, E.-M. Cyanobacterial oxygenic photosynthesis is protected by flavodiiron proteins. *Life* **5**, 716–743 (2015).
66. Latifi, A., Ruiz, M. & Zhang, C.-C. Oxidative stress in cyanobacteria. *FEMS Microbiol. Rev.* **33**, 258–278 (2009).
67. Kelman, D., Ben-Amotz, A. & Berman-Frank, I. Carotenoids provide the major antioxidant defence in the globally significant N2-fixing marine cyanobacterium *Trichodesmium*. *Environ. Microbiol.* **11**, 1897–1908 (2009).
68. Chen, H. Y. S., Bandyopadhyay, A. & Pakrasi, H. B. Function, regulation and distribution of IsiA, a membrane-bound chlorophyll a-antenna protein in cyanobacteria. *Photosynthetica* **56**, 322–333 (2018).
69. Michel, K. P. & Pistorius, E. K. Adaptation of the photosynthetic electron transport chain in cyanobacteria to iron deficiency: the function of IdiA and IsiA. *Physiol. Plant.* **120**, 36–50 (2004).
70. Shi, T., Sun, Y. & Falkowski, P. G. Effects of iron limitation on the expression of metabolic genes in the marine cyanobacterium *Trichodesmium erythraeum* IMS101. *Environ. Microbiol.* **9**, 2945–2956 (2007).
71. Boatman, T. G., Oxborough, K., Gledhill, M., Lawson, T. & Geider, R. J. An integrated response of *Trichodesmium erythraeum* IMS101 growth

and photo-physiology to iron, $CO_2$, and light intensity. *Front. Microbiol.* **9**, 624 (2018).
72. Hutchins, D. A., Fu, F.-X., Webb, E. A., Walworth, N. & Tagliabue, A. Taxon-specific response of marine nitrogen fixers to elevated carbon dioxide concentrations. *Nat. Geosci.* **6**, 790–795 (2013).
73. Garcia, N. S. et al. Interactive Effects of Irradiance and $CO_2$ on $CO_2$ Fixation and $N_2$ Fixation in the Diazotroph *Trichodesmium erythraeum* (Cyanobacteria)[1]. *J. Phycol.* **47**, 1292–1303 (2011).
74. Geider, R. J., Moore, C. M. & Ross, O. N. The role of cost–benefit analysis in models of phytoplankton growth and acclimation. *Plant Ecol. Divers.* **2**, 165–178 (2009).
75. Allen, J. F. Cyclic, pseudocyclic and noncyclic photophosphorylation: new links in the chain. *Trends Plant Sci.* **8**, 15–19 (2003).
76. Kranz, S. A., Sültemeyer, D., Richter, K.-U. & Rost, B. Carbon acquisition by *Trichodesmium*: the effect of $pCO_2$ and diurnal changes. *Limnol. Oceanogr.* **54**, 548–559 (2009).
77. Barcelos e Ramos et al. Effect of rising atmospheric carbon dioxide on the marine nitrogen fixer *Trichodesmium*. *Glob. Biogeochem. Cycles* **21**, GB2028 (2007).
78. Kranz, S. A., Eichner, M. & Rost, B. Interactions between CCM and $N_2$ fixation in *Trichodesmium*. *Photosynth. Res.* **109**, 73–84 (2011).
79. Baker, N. R., Harbinson, J. & Kramer, D. M. Determining the limitations and regulation of photosynthetic energy transduction in leaves. *Plant Cell Environ.* **30**, 1107–1125 (2007).
80. Inomura, K., Wilson, S. T. & Deutsch, C. Mechanistic model for the coexistence of nitrogen fixation and photosynthesis in marine *Trichodesmium*. *mSystems* **4**, e00210–e00219 (2019).
81. Nicholson, D. P., Stanley, R. H. R. & Doney, S. C. A phytoplankton model for the allocation of gross photosynthetic energy including the trade-offs of diazotrophy. *J. Geophys. Res. Biogeosci.* **123**, 1796–1816 (2018).
82. Staal, M., Meysman, F. J. & Stal, L. J. Temperature excludes $N_2$-fixing heterocystous cyanobacteria in the tropical oceans. *Nature* **425**, 504–507 (2003).
83. Wolf-Gladrow, D. & Riebesell, U. Diffusion and reactions in the vicinity of plankton: a refined model for inorganic carbon transport. *Mar. Chem.* **59**, 17–34 (1997).
84. Pahlow, M., Dietze, H. & Oschlies, A. Optimality-based model of phytoplankton growth and diazotrophy. *Mar. Ecol. Prog. Ser.* **489**, 1–16 (2013).
85. Mahowald, N. M. et al. Atmospheric iron deposition: global distribution, variability, and human perturbations. *Annu. Rev. Mar. Sci.* **1**, 245–278 (2009).

## Acknowledgements

National Natural Science Foundation of China to Y-W.L. (Grants 42376140 and 42076153), China Scholarship Council and MEL PhD fellowship to W.L., and Grant Agency of the Czech Republic to O.P. (Grant 23-06593S) and to M.E. (Grant 24-11363S). This work was supported by a grant from the Simons Foundation (LS-ECIAMEE-00001549, Inomura). We thank these foundations for their support.

## Author contributions

Y-W.L. originated the concept for the study. Y-W.L. and W.L. designed the numerical model. W.L. coded the initial version of the model and performed numerical modeling. W.L., M.E., O.P., K.I., F.Z., and Y-W.L. analyzed results and improved the numerical model. W.L. wrote the original draft, which was reviewed and edited by all the co-authors.

## Competing interests

The authors declare no competing interests.

## Additional information

**Supplementary information** The online version contains supplementary material available at https://doi.org/10.1038/s43247-026-03344-y.

**Correspondence** and requests for materials should be addressed to Ya-Wei Luo.

**Peer review information** *Communications Earth and Environment* thanks Nathan S Garcia and the other anonymous reviewer(s) for their contribution to the peer review of this work. Primary handling editors: Giulia Faucher and Alice Drinkwater. [A peer review file is available].